Crystallographic Study of Glu58Ala RNase T1·2′-Guanosine Monophosphate at 1.9-Å Resolution[†,‡]

Jurgen Pletinckx,[*,§] Jan Steyaert,[§] Ingrid Zegers,[§] Hui-Woog Choe,[‖] Udo Heinemann,[‖] and Lode Wyns[§]

Instituut voor Moleculaire Biologie, Laboratorium Ultrastructuur, Vrije Universiteit Brussel, Paardenstraat 65, B-1640 Sint-Genesius-Rode, Belgium, and Institut für Kristallographie, Freie Universität Berlin, Takustrasse 6, D-1000 Berlin 33, Germany

Received April 12, 1993; Revised Manuscript Received July 12, 1993[⊛]

ABSTRACT: Glu58 is known to participate in phosphodiester transesterification catalyzed by the enzyme RNase T1. For Glu58 RNase T1, an altered mechanism has been proposed in which His40 replaces Glu58 as the base catalyst [Steyaert, J., Hallenga, K., Wyns, L., & Stanssens, P. (1990) *Biochemistry 29*, 9064–9072]. Glu58Ala Rnase T1 has been cocrystallized with guanosine 2′-monophosphate (2′-GMP). The crystals are of space group $P2_1$, with one molecule per asymmetric unit (a = 32.44 Å, b = 49.64 Å, c = 26.09 Å, $\beta = 99.17°$). The three-dimensional structure of the enzyme was determined to a nominal resolution of 1.9 Å, yielding a crystallographic R factor of 0.178 for all X-ray data. Comparison of this structure with wild-type structures leads to the following conclusions. The minor changes apparent in the tertiary structure can be explained by either the mutation of Glu58 or by the change in the space group. In the active site, the extra space available through the mutation of Glu58 is occupied by the phosphate group (after a reorientation) and by a solvent molecule replacing a carboxylate oxygen of Glu58. This solvent molecule is a candidate for participation in the altered mechanism of this mutant enzyme. Following up on a study of conserved water sites in RNase T1 crystallized in space group $P2_12_12_1$ [Malin, R., Zielenkiewicz, P., & Saenger, W. (1991) *J. Mol. Biol. 266*, 4848–4852], we investigated the hydration structure for four different packing modes of RNase T1. Several of the water molecules as well as the cation binding site that are conserved in space group $P2_12_12_1$ are absent in structures in other space groups.

Ribonuclease T1 (RNase T1,[1] EC 3.1.27.3) of the slime mould *Aspergillus oryzae* is the best known representative of a large family of microbial ribonucleases (Hill *et al.*, 1983). It depolymerizes single-stranded RNA by specifically breaking the P–O5′ bond of GpN sequences (Sato & Egami, 1957). The structure and function of the enzyme have been investigated using a variety of chemical modification, kinetic, spectroscopic, and X-ray crystallographic methods.

Secondary structure elements comprise an α-helix and two antiparallel β-sheets, connected through a series of wide loops (Heinemann & Saenger, 1982; Arni *et al.*, 1988) (Figure 1). The structure is stabilized by two disulfide bridges. The residues implicated in catalysis are anchored in the major B-sheet, while substrate recognition is performed by residues in loop regions.

Mechanisms for the transesterification reaction catalyzed by RNase T1 generally include the proposal that Glu58 and His92 provide general base/general acid assistance, with Tyr38, Arg77, and His40 in accessory roles (Heinemann & Saenger, 1982). The role of Glu58 was challenged by the observation that mutants substituted at position 58 retain high residual activity, whereas substitutions for His40 reduce the turnover number by 3 orders of magnitude. A revised mechanism was proposed in which His40, and not Glu58, is engaged in catalysis as the general base (Nishikawa *et al.*, 1987). A recent study of the pH profiles of wild-type RNase T1 and of several single-site mutants for the transesterification of model compounds confirms the attribution of the role of general base to Glu58 and suggests that the protonated His40 imidazole group participates in electrostatic stabilization of

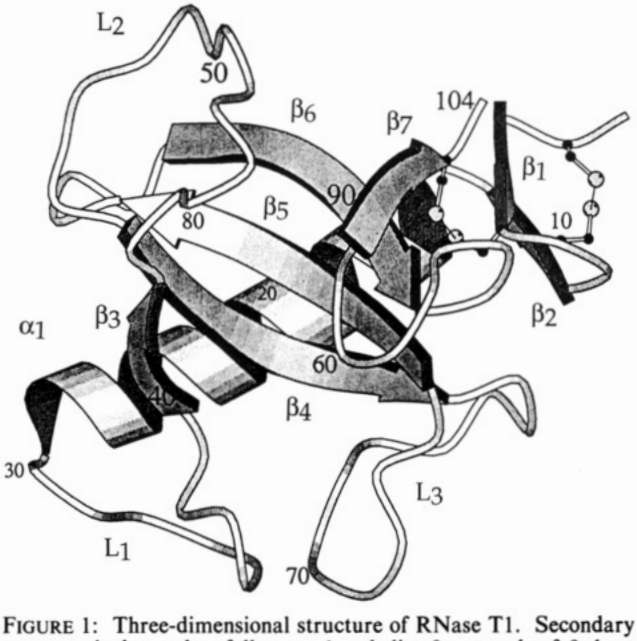

FIGURE 1: Three-dimensional structure of RNase T1. Secondary structure is denoted as follows: α1, α-helix; βn, strands of β-sheet structure; Ln, loops. Drawn by Molscript (Kraulis, 1991). Residue numbers indicate the beginning and end of secondary structure elements.

[†] This work was supported by the Vlaams Actieprogramma Biotechnologie, the Deutsche Forschungsgemeinschaft, and the Fonds der Chemischen Industrie. J. P. and I. Z. are recipients of a grant from the Instituut voor Wetenschappelijk Onderzoek in de Nijverheid; J. S. is a research assistant of the Nationaal Fonds voor Wetenschappelijk Onderzoek.

[‡] Atomic parameters for the final structure were deposited at the Protein Data Bank, entry 1RLA.

* To whom correspondence should be addressed.

§ Vrije Universiteit Brussel.

‖ Freie Universität Berlin.

⊛ Abstract published in *Advance ACS Abstracts,* February 1, 1994.

[1] Abbreviations: 2′-GMP, guanosine 2′-monophosphate; GpA, guanylyl-2′,5′-adenosine; PEG, polyethylene glycol; pGp, guanosine 3′,5′-biphosphate; RNase T1, *Aspergillus oryzae* ribonuclease T1; wt, wild type.

0006-2960/94/0433-1654$04.50/0

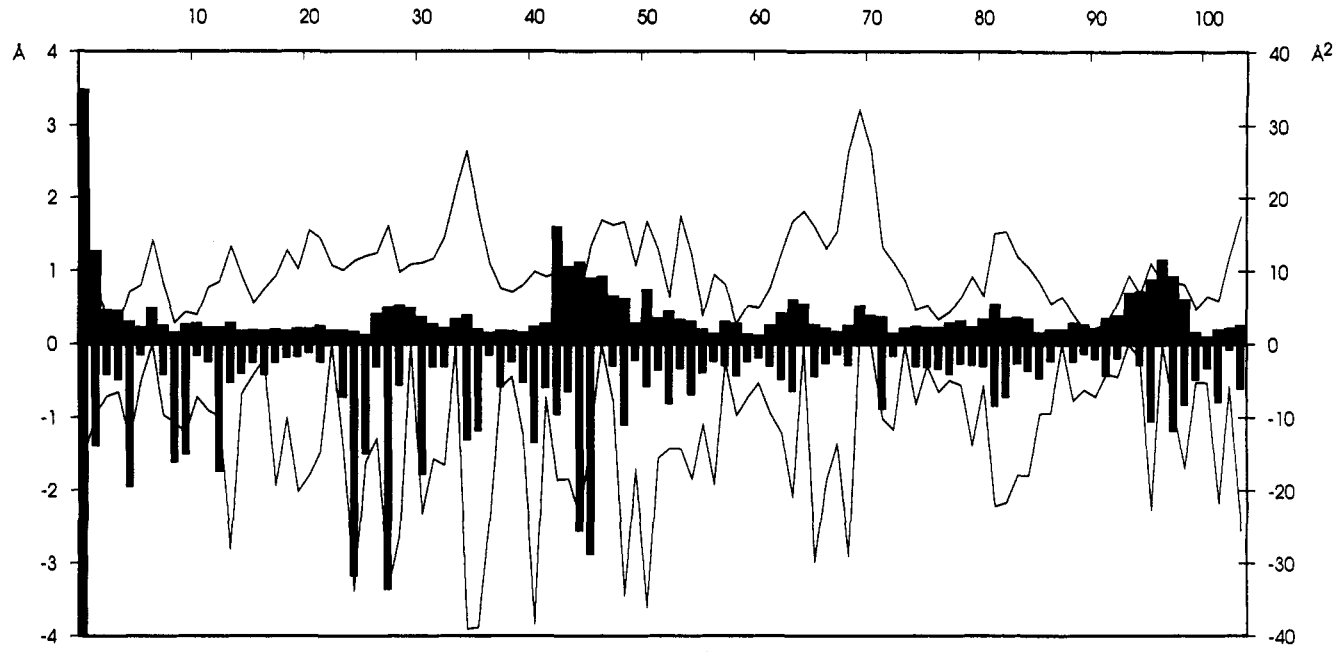

FIGURE 2: Mean temperature factors for Glu58Ala RNase T1 (full line, Å²) and the rms deviations between Glu58Ala RNase T1·GMP and native RNase T1 (Martinez-Oyanedel *et al.*, 1991) (bar graph, Å) for main-chain atoms (above the axis) and for side-chain atoms (below the axis).

the transition state in wild-type enzyme (Steyaert *et al.*, 1990). The high residual activity of the Glu58Ala-substituted enzyme has been explained by the ability of His40 to adopt the function of general base. The pH dependence of the catalytic parameters of Glu58Ala RNase T1 are indicative of an alternate mechanism in which His40 and His92 act as base and acid catalysts, respectively.

For RNase T1, up to 16 different X-ray structures have been reported, with the focus on different substrate analogue complexes and on mutants in the active site of the enzyme [for review, see Heinemann and Polyakov (1992)]. Most of these structures were derived from isomorphous crystals in space group $P2_12_12_1$ (approximate cell dimensions for crystals of this "canonical" space group are a = 50 Å, b = 46 Å, c = 41 Å).

Here we present the crystal structure of Glu58Ala RNase T1 complexed with the specific inhibitor 2′-GMP in space group $P2_1$. In analyzing this protein structure, we focus on the structural aspects of the change in enzyme mechanism that is associated with the Glu58Ala mutation. We also investigate the implications of the difference in space group on the structure of the protein and its hydration shell.

MATERIALS AND METHODS

Crystallization and Data Collection. The overproduction of Glu58Ala RNase T1 as a secretory protein in *Escherichia coli* and its purification have been described previously (Steyaert *et al.*, 1990). Crystals were grown in a sitting drop experiment by equilibrating a solution of 1.5% by weight recombinant RNase T1, 0.125% by weight 2′-GMP against a solution of 55% by volume 2-methyl-2,4-pentanediol, 20 mM sodium acetate, and 2 mM calcium acetate at pH 4.2. The protocol yielded two crystal forms of space groups $P2_1$ and $P2_12_12_1$, respectively. From crystals belonging to space group $P2_1$, two series of structure amplitudes were collected independently of each other on an Enraf Nonius FAST area detection system at room temperature, using Ni-filtered Cu Kα radiation (λ = 1.54178 Å) from a FR571 rotating anode generator (55 kV, 65 mA, focal spot size 0.2 × 2.0 mm²). The

Table 1: Crystal Data and Summary of Refinement Results

Crystal Parameters	
space group	$P2_1$
lattice constants	a = 32.44 Å b = 49.64 Å c = 26.09 Å β = 99.75°
unit cell volume	41406 Å³
starting model	free RNase T1
resolution (Å)	8–1.9
no. of reflections used	5580
final R factor	0.178
mean error in atomic positions (Å)	0.2
rms density of final $F_o - F_c$ map (electrons/Å³)	0.093
Root Mean Square Deviations from Ideal Stereochemistry (Target Restraints)	
bond distance (Å)	0.024 (0.020)
angle distance (Å)	0.060 (0.050)
planarity restraints (Å)	0.013 (0.015)
chiral center restraints (Å³)	0.250 (0.150)
Average Temperature Factors (Å²)	
main-chain protein atoms	10.0
side-chain protein atoms	13.6
inhibitor atoms	9.2
conserved water molecules	19.5
other solvent atoms	31.3
sodium atom	19.4

cell dimensions, a = 32.44 Å, b = 49.64 Å, c = 26.09 Å, and β = 99.75°, were obtained by refinement against 200 reflections. The two data sets contained 4803 and 4886 reflections, respectively, and were merged and scaled to give 5659 unique reflections to a resolution of 1.9 Å. [R_{merge} (F^2) = $(\sum_h\sum_i(<|F_h|> - |F_i|^2/\sum_h\sum_i|F_{h,i}|^2)^{1/2}$ = 0.069.]

Molecular Replacement and Refinement. The present crystal is not isomorphous to the crystals of any hitherto solved RNase T1 structure. The starting model (the protein atoms of the crystal structure of RNase T1 with free recognition site; Martinez-Oyanedel *et al.*, 1991) has been positioned in unit cell $P2_1$ using molecular replacement methods (Crowther & Blow, 1967; Crowther, 1972) as implemented in the program

Table 2: Possible Intermolecular Hydrogen Bonds

symmetry operation	bond		bond distance (Å)
x,y,1+z	3 O	97 N	2.98
	4 OH	98 Nδ2	2.62
	13 O	98 Oδ1	3.06
	13 Oγ	98 Oδ1	2.67
1+*x,y,z*	25 Nζ	49 Oδ1	2.84
	25 Nζ	49 Oδ2	2.99
1-*x*,*y*+1/2,-*z*	1 N	29 Oδ1	2.70
1-*x*,*y*+1/2,1-*z*	8 N	31 Oδ2	2.65
	9 Oδ1	30 O	3.10
	63 Oγ	30 O	2.65
-*x*,*y*-1/2,-*z*	53 Oγ	104 O	3.16
	83 Nδ2	104 O	3.08

package MERLOT[2] (Fitzgerald, 1988). This resulted in a model with an initial *R* factor of 0.52. Rigid-body refinement of this model with the program CORELS (Sussman *et al.*, 1977; Sussman, 1985) reduced the *R* factor to 0.45. Initially, constrained–restrained least-squares refinement (program CORELS) was used to refine the structure to an *R* factor of 0.32. Further refinement was achieved through stereochemically restrained least-squares refinement in the fast Fourier transformation version PROFFT (Finzel, 1987; Sheriff, 1987) of the program PROLSQ (Hendrickson & Konnert, 1980; Hendrickson, 1985), combined with model building sessions (program FRODO, version 4.4; Jones, 1978, 1985).

Inspection of the difference electron density indicated the presence of an inhibitor in the active site. All atoms of 2′-GMP were added to the structure. Spherically shaped difference densities at geometrically plausible positions in the structure were interpreted as water molecules. A dense peak near His92 and Ala95 was interpreted as a sodium ion. The refinement converged at an *R* factor of 0.178. For the final structure, the mean error in atomic position was estimated by the method of Luzzati (1952) to be <0.20 Å.

Identification of Conserved Solvent Sites. For comparison of the water sites in different RNase T1 structures (Table 5), the various structures were superimposed onto the present structure of Glu58Ala RNase T1 by a least-squares fit of the Cα atoms using XPLOR (Brünger *et al.*, 1987). Water molecules within a common sphere of 1-Å diameter were considered "conserved" (Malin *et al.*, 1991).

RESULTS

Crystallization. The protocol we used to grow crystals (Materials and Methods) yielded two different crystal species of space group $P2_1$ and $P2_12_12_1$, respectively. The same protocol has previously been used to grow crystals for wild-type enzyme and some mutants, either native or complexed with various ligands; all of these in the canonical space group $P2_12_12_1$ [see Heinemann and Polyakov (1992) for review]. The crystals in space group $P2_1$ diffracted to a resolution of 1.9 Å; these crystals were used in the structure determination of Glu58Ala RNase T1. The crystals in space group $P2_12_12_1$ diffracted poorly and have not been considered for data collection.

General Structure. The final structure contains 893 atoms, including 768 fully occupied protein atoms, five side-chain atoms in partially occupied alternate positions, 24 inhibitor atoms, a sodium ion, and 90 water molecules. For Oγ of Ser13 and Ser37, for Cγ1 and Cγ2 of Val78, and for Cδ2 of Leu26, two conformations have been identified. No position could be assigned to the side-chain atoms of Tyr45 beyond Cδ1 and Cδ2. The atomic parameters were deposited at the Protein Data Bank (entry 1RLA). The residue numbering is 1–104 for the protein itself, 105 for 2′-GMP, 106 for the sodium ion, and 107–196 for water molecules (with increasing numbers indicating higher temperature factors).

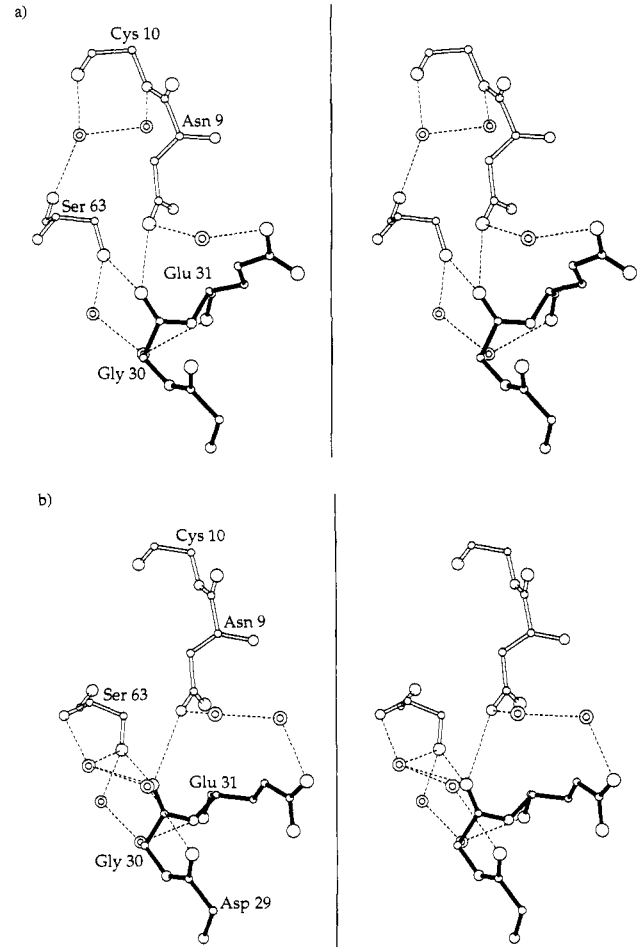

FIGURE 3: Comparison of the environment of Gly30 in Glu58Ala RNase T1·2′-GMP (a) and in native RNase T1 (Martinez-Oyanedel *et al.*, 1991) (b). (Side chain of Asp29 omitted for clarity; atoms generated by crystal symmetry are indicated by hollow bonds.)

Statistical details on the refinement, the geometry, and the temperature factors of the final structure are gathered in Table 1. According to the program DSSP (Kabsch & Sander, 1983), all secondary structure elements found throughout other structures of RNase T1 (Figure 1) are preserved in the Glu58Ala structure. The only notable difference in tertiary structure concerns the amino-terminal residues Ala1 and Cys2. These have been rotated by 60° around the N3–Cα3 bond relative to the rest of the structure. Smaller conformational changes occur mainly in the guanosine binding site and the loop regions (Figure 2). Similar structural variations were previously observed for other RNase T1 structures.

Packing. The change in space group from $P2_12_12_1$ to $P2_1$ is reflected in different direct intermolecular contacts (Table 2). The contacts between the carbonyl oxygen of Gly30 and the side chains of Asn9 and Ser63 of a neighboring molecule are a notable exception. The latter contacts are observed in $P2_1$ as well as in $P2_12_12_1$ (Figure 3 and Table 2).

Upon comparing the present structure with previous structures, we observe significant differences in the confor-

[2] All programs were executed on a VAXserver 3300 in cluster with a VAXstation 3100 or on a CRAY YMP. Model building and visual inspection were performed on a graphics system Evans and Sutherland PS390 A+.

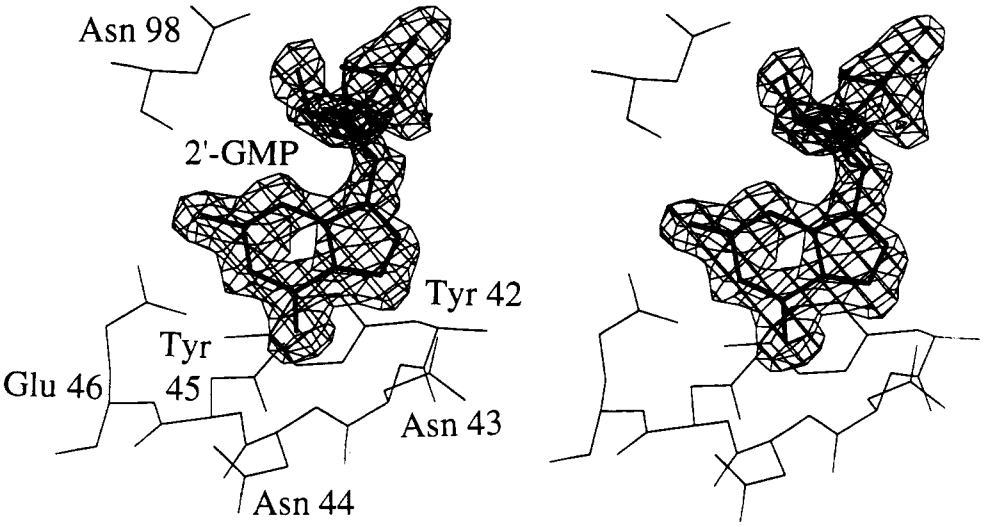

FIGURE 4: Stereoview of the difference ($F_o - F_c$) electron density for the inhibitor. The map shown was computed after 12 refinement cycles with the final coordinate set from which 2′-GMP was omitted.

mation of some surface residues (e.g., Lys25, Glu31, Asp49). It is uncertain whether these differences are caused by the change in packing. In the various RNase T1 structures, the side-chain atoms of these residues have high temperature factors, if they fit in any electron density at all. Note that various conformations have been observed for these residues, even among structures in the same space group. The change in conformation of the amino terminus (see Results), on the other hand, may result from the different packing. In the present structure, a hydrogen bond is formed between the terminal amino group and the carboxyl group of Asp29 of a neighboring molecule. In the canonical space group, intermolecular hydrogen bonds are formed between the terminal amino group and the main chain carbonyl oxygens of His92, Ala95, and Gly97 of a neighboring molecule.

Inhibitor Binding. In the present structure of Glu58Ala RNase T1, one molecule of the specific inhibitor 2′-GMP is bound to the primary nucleotide binding site of the enzyme. The guanine moiety of the inhibitor is located in the guanine recognition pocket; the phosphate group is bound to the catalytic site. All inhibitor atoms are clearly defined (Figure 4). The glycosidic bond adopts the syn conformation; the ribose forms a C4′-exo envelope (Table 3; Altona & Sundaralingam, 1980). The intermolecular contacts that define the guanine specificity of RNase T1 (Heinemann & Saenger, 1982; Arni *et al.*, 1988) are present with only one exception. The hydrogen bonds between the guanine moiety and residues 42–46 and 98 are listed in Table 3. In addition, the base stacks onto the phenolic group of Tyr42. The notable exception concerns the side chain of Tyr45. In previously described structures, this side chain closes the primary binding site like a lid if guanine is bound. In the present structure, however, it is impossible to define a position for the atoms of the ring atoms beyond Cδ1 and Cδ2. For the visible part of the side chain, the temperature factors rise steeply: Cα, 4.7 Å^2; Cβ, 15.3 Å^2; Cγ, 26.0 Å^2; Cδ1 and Cδ2, 25.9 Å^2.

In Glu58Ala RNaseT1·2′-GMP, the position that atom Oε1 of Glu58 takes in the corresponding wild-type complex is occupied by a well-defined water molecule (Wat 220). In addition, the orientation of the phosphate group has drastically changed in the present structure (Figure 5). A similar reorientation in the wild type·2′-GMP complex would lead to a steric clash between atom O3P of the inhibitor and atom Oε2 of Glu58. Despite this change in orientation, the contacts between the side chains that make up the catalytic site (Tyr38, His40, Arg77, and His92) and the phosphate moiety of the bound inhibitor are similar to wild-type enzyme (Figure 5 and Table 3). The new orientation causes the side chain of Arg77 to be within hydrogen-bonding distance to the phosphate group (see Table 3). The side chain of His40 is tilted by 10° across the Cβ–Cγ axis relative to its usual position. This does not impede the contacts with the phosphate group. Finally, an additional hydrogen bond is observed between atom O3P of the phosphate group and the water molecule (220) that

Table 3: Inhibitor Conformation and Possible Hydrogen Bonds between Protein and Inhibitor

backbone torsion angles (deg)	E58A	wt
O5′-C5′-C4′-C3′ (γ)	156	65
C5′-C4′-C3′-O3′ (δ)	83	152
C5′-C4′-C3′-C2′	−170	−94
C4′-C3′-C2′-O2′	−71	−161
C3′-C2′-O2′-P	−122	−122

glycosyl torsion angle (deg)	E58A	wt
O1′-C1′-N9-C4 (χ)	75 (*syn*)	55 (*syn*)

pseudorotation angles (deg)[a]	E58A	wt
C4′-O1′-C1′-C2′ (τ_0)	−21	−25
O1′-C1′-C2′-C3′ (τ_1)	39	−12
C1′-C2′-C3′-C4′ (τ_2)	−40	40
C2′-C3′-C4′-O1′ (τ_3)	28	−55
C3′-C4′-O1′-C1′ (τ_4)	−5	51
P	168 (C2′-*endo*)	44 (C4′-*exo*)

inhibitor atom	protein atom	distance (Å)
N1	46 Oε1	2.69
N2	98 O	2.87
	46 Oε2	2.60
N3		
O6	44 N	2.69
	45 N	3.00
N7	43 N	2.96
O1′		
O3′	98 Oδ1	2.91
	222 O	3.00
O5′	239 O	2.61
O1P	38 OH	2.48
	222 O	3.07
O2P	77 Nε	3.09
	77 Nη2	3.16
	92 Nε2	2.75
O3P	40 Nε2	2.73
	220 O	2.80

[a] Altona and Sundaralingam (1972).

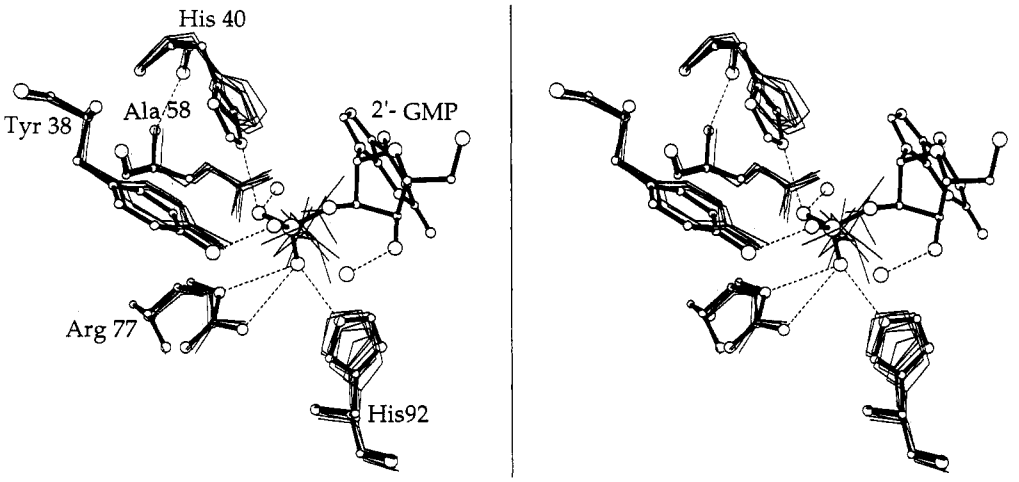

FIGURE 5: Comparison of the catalytic sites of Glu58Ala RNase T1·2′-GMP (ball and stick model) and of wild-type RNase T1 in native state and complexed with vanadate, GpG, pGp, 2′-GMP, and AMP (line drawings). For the latter four structures, only the relevant phosphate group of the inhibitor is displayed. The structures were superimposed by a least-squares fitting of the Cα atoms.

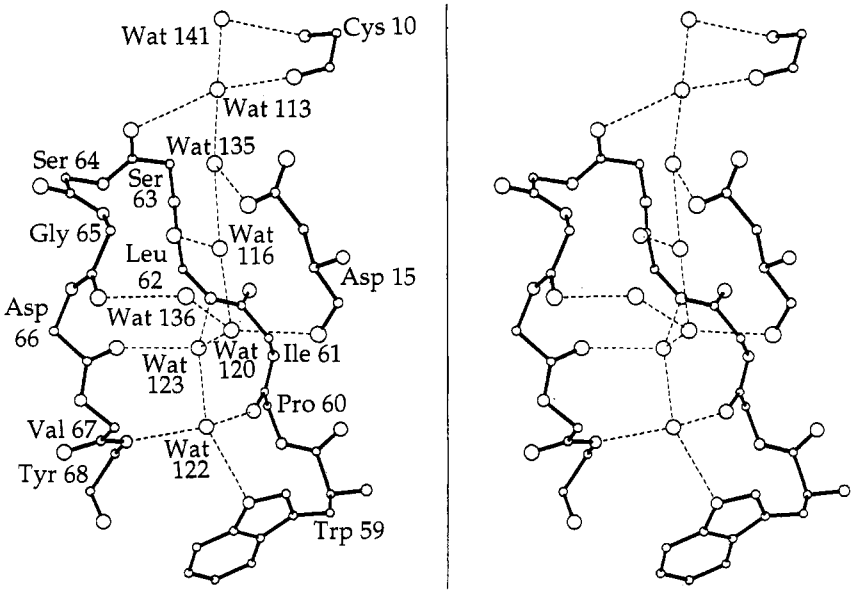

FIGURE 6: Stereoview of a stretch of conserved solvent sites and the part of the protein interacting with these water molecules. For clarity, only the side chains of Asp15 and Trp59 are displayed. The water molecules are numbered according to the list of conserved solvent sites, not following the actual residue number.

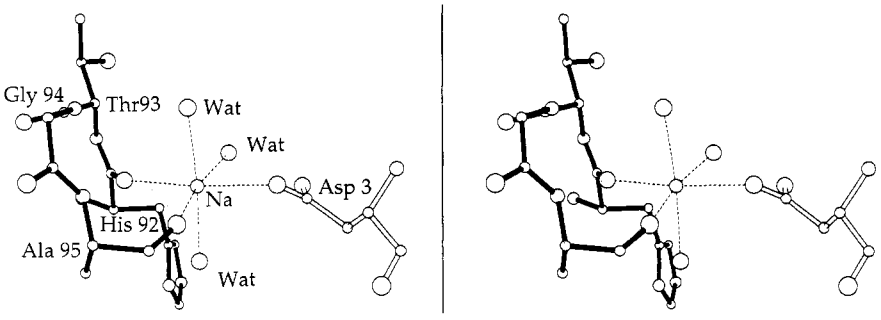

FIGURE 7: Stereoview of the cation binding site in Glu58Ala RNase T1. (Hollow bonds indicate atoms generated through crystal symmetry.)

structurally replaces atom Oε1 of Glu58 in the mutant.

Hydration. In the present structure of Glu58Ala RNase T1, a total of 90 water molecules have been located in the asymmetric unit. Surprisingly, only 16 out of the 30 water molecules that are structurally conserved (Materials and Methods) in canonical space group $P2_12_12_1$ (Malin *et al.*, 1991) are observed in the present structure in $P2_1$ (Table 4). We expanded the study of Malin *et al.* by including four additional structures in four more space groups[3] (Table 5). For clarity, we will discuss all the conserved water molecules that have been identified previously by Malin *et al.* following their arbitrary numbering (sites 106–135; this numbering bears no relation to the PDB files, where water molecules are ordered

[3] The packing of the His40Lys·2′-GMP structure (Zegers et al., 1992), although crystallized in spacegroup $P2_1$, very much resembles the packing in the canonical space group through noncrystallographic symmetry. Therefore, this structure has been considered as belonging to the canonical space group.

Table 4: Coordination Distances (Å) of Conserved Solvent Sites for RNase T1 Crystal Structures in Four Different Space Groups

site no.	hydrogen bond partner	RNase T1 E58A·2′-GMP	wt·pGp	H92A·PEG	H92A·PO$_4^{3-}$	wt·2′-GMP	site no.	hydrogen bond partner	RNase T1 E58A·2′-GMP	wt·pGp	H92A·PEG	H92A·PO$_4^{3-}$	wt·2′-GMP
106	2 N					2.99	123	62 N	3.05	3.10	2.83	3.08	3.26
107	1 O		3.05			2.62		66 O	2.71	2.63	2.50	2.68	2.51
	3 N		2.92			3.15		120 O	2.69	2.79	2.88	3.11	3.01
108	2 O		2.70	2.93	2.83	2.96		122 O	2.93	2.75	2.63	2.87	2.59
	5 Oγ		2.70				124	21 O	2.72	2.81		2.74	2.84
	104 Oxt		2.60	2.84	2.87	2.47	125	31 O	2.96	2.65	2.67	2.84	2.82
109	89 N	2.95	3.09		3.27	2.87		126 O	2.62	2.76	2.60	2.70	2.89
	89 O				3.36	3.23		128 O					2.38
	102 Oε2		3.33		2.93		126	27 Nδ1	2.75	2.70	3.17	3.09	
110	13 O		2.87	3.09		2.77		125 O	2.62	2.76	2.60	2.70	2.89
	17 Oγ		3.31			3.06	127	29 O					3.20
111	6 O	3.05	2.95	2.63	2.93	3.21		30 O					3.40
	9 Oδ1	3.27	3.07	3.11	3.30	3.11	128	125 O	2.62				2.38
	76 Oδ1	2.72	2.76	2.60	2.71	2.72	129	31 Oε1					2.59
	93 Oγ1	2.80	2.86	2.87		2.54	130	32 Oγ					3.49
	112 O	2.80	3.17			2.85		37 O					3.30
112	8 N	2.95	3.11			3.40		39 O	2.87		2.88		3.03
	111 O	2.80	3.17			2.85		132 O			2.72		2.85
113	10 O	2.68				2.92	131	35 N		3.15		3.12	3.37
	63 O	3.17				2.91		36 N	3.16	3.01	3.23	2.86	3.03
	135 O	3.46				3.12		68 OH	2.77	3.04	2.74		3.05
114	63 N	3.19	3.16		3.10	3.25		140 O	3.14	3.34		2.91	
	63 Oγ	3.32	3.15			3.23	132	130 O			2.72		2.85
	134 O	3.20			2.93	3.16	133	102 N	2.76	2.92	3.07	2.96	3.01
	138 O	2.87	2.87		2.73	2.88	134	75 N	3.02			2.84	2.84
115	10 O					2.45		114 O	3.20			2.93	3.16
	15 Oδ2					3.05	135	15 Oδ1					3.23
	121 O					3.45		15 Oδ2	2.96				2.94
116	62 O	2.79	2.61	2.54	2.60	2.87		113 O	3.46				3.12
	120 O	2.78	2.83	3.25	2.75	2.67		116 O	2.81				2.88
	135 O	2.81		3.11		2.88	136	65 O	3.24	2.69		3.28	3.48
117	12 Oγ					3.04		120 O	3.11	2.72		2.79	2.96
	15 Oδ1					2.81	137	69 N	3.05	2.78	3.16	3.06	3.21
	15 Oδ2					2.99		70 O	2.57		2.82	3.05	3.00
	118 O					3.34	138	61 O	2.73	2.68	2.59	2.64	2.58
	121 O					2.78		73 O	2.66	2.64	3.13	2.78	2.66
118	14 Oγ					2.72		76 N	3.29	3.03	3.33	3.24	3.06
	15 N					3.32		114 O	2.87	2.87		2.73	2.88
	15 Oδ1					2.64	139	53 N	2.96	2.92	3.01	2.83	3.14
	117 O					3.34		53 Oγ	2.90	3.27	2.90	2.96	3.26
	119 O					2.62		85 Oε1	2.61	2.63	2.90	3.46	2.29
119	18 Oγ				2.79	2.91	140	35 N	2.98	2.98	3.36	2.75	3.09
	118 O					2.62		35 Oγ		3.39	3.16	2.86	
120	15 O	2.95	2.72	3.03	2.85	2.53		71 O	3.14	3.00	3.31	2.87	2.87
	116 O	2.78	2.83	3.25	2.75	2.63		131 O	3.14	3.34		2.91	
	123 O	2.69	2.79	2.88	3.11	3.01	141	51 N	3.04	2.69	2.67		2.94
121	115 O					3.45		51 Oγ		2.84	3.19		3.27
	117 O					2.78		87 O	2.56	2.81	3.06		2.64
122	59 Nε1	2.96	3.24	2.99	3.07	3.08	142	32 Oγ1	3.13	3.34			
	60 O		2.77	2.96	2.83	2.83		34 O	2.64	2.77	2.58		
	68 N	2.84	2.85	2.76	2.83	2.78		37 Oγ	3.21	3.43			
	123 O	2.93	2.75	2.63	2.87	2.59							

Table 5: Crystal Structures Used for Determination of Conserved Water Sites

structure	space group	resolution	no. of waters	reference
E58A RNase T1·2′-GMP	$P2_1$	1.9	90	present study
H92A RNase T1·PO$_4^{3-}$	$P2_12_12_1$	1.8	81	Koellner *et al.* (1992)
H92A RNase T1-PEG	$P2_12_12_1$	2.2	70	Koellner *et al.* (1992)
wt RNase T1·pGp	$I23$	1.9	120	Lenz *et al.* (1993)
wt RNase T1·various[a]	$P2_12_12_1$	1.9[a]	91[a]	Malin *et al.* (1991)[a]

[a] This article contains an analysis of conserved water sites for four structures in the canonical space group, with resolutions ranging between 1.8 and 1.9 Å and the number of water molecules ranging between 91 and 185.

with ascending temperature factors). Seven more conserved solvent sites have been identified in the present study (Table 4) and are numbered accordingly from 136 to 142.

From our investigation, it appears that only part of the conserved water sites in $P2_12_12_1$ (Malin *et al.*, 1991) are consistently occupied in other space groups. In total, we identified 25 water molecules that are structurally conserved throughout the different packing modes (Table 4). Among these, sites 108, 109, 110, 124, 130, 133, 137, 139, 143, and 144 do not contact any other conserved solvent site. The remaining sites occur in clusters of two (sites 111–112, 125–126, and 131–140) or three molecules (sites 114, 134, and 138). A final cluster deserves special mention (Malin *et al.*, 1991): a long stretch of solvent sites starts at the side chain

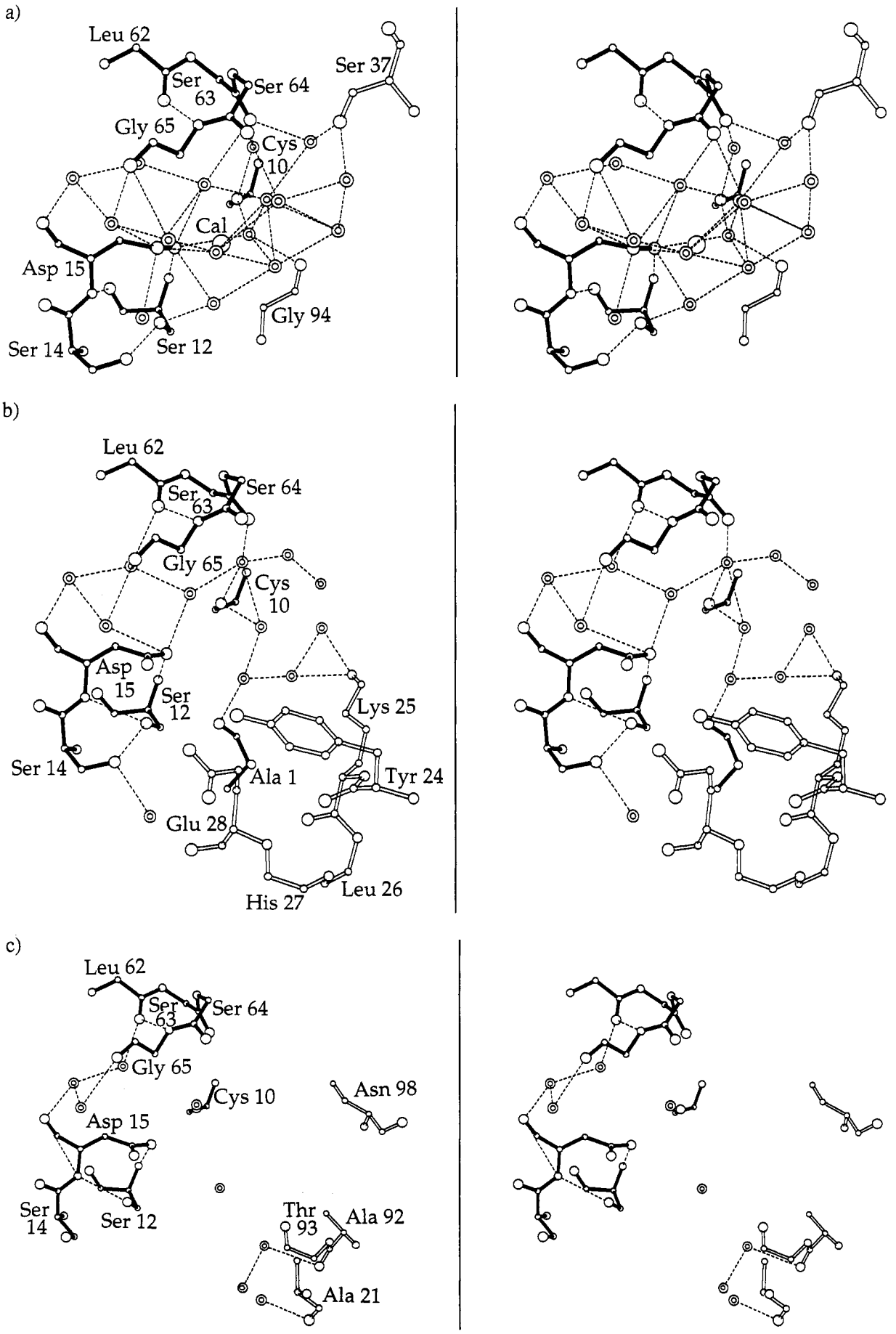

FIGURE 8: Comparison of the cation binding site of space group $P2_12_12_1$ (a) in RNase T1·2′-GMP (Arni, 1988), (b) in Glu58Ala RNase T1·GMP, and (c) in His92Ala RNase T1·PO^{4-} (Koellner, 1992). Residues 11 and 13 and the side chains of residues 10, 14, and 62–64 are deleted for clarity; atoms generated through crystal symmetry are indicated by hollow bonds.

of Trp59 and continues via sites 122–123–120–116–135, with a branch from site 120 to site 136 (Figure 6).

New Cation-Binding Site. In the present structure, one peak in the difference density was identified as a sodium ion. The ion shows 6-fold coordination in a nearly perfect octahedron, with very short ligand distances. Its ligands include the backbone carbonyl oxygen of His92 and Ala95, along with three water molecules and a side-chain carboxyl oxygen from a neighboring molecule. Ligand distances are 2.52 ± 0.08 Å. The spatial arrangement around the sodium ion is shown in Figure 7. The previously described cation-binding site near Asp15 (Koepke *et al.*, 1989) is not occupied, and there is no evidence of the hydrogen-bonding network associated with the site in the canonical space group (Figure 8). This network connected the calcium binding site to the stretch of solvent sites mentioned above.

DISCUSSION

The crystal structure of the Glu58Ala mutant of RNase T1 complexed with 2′-GMP has been analyzed in space group $P2_1$ at a resolution of 1.9 Å.

If compared with the RNase T1·2′-GMP complex (Arni *et al.*, 1988), the extra space available after removal of the Glu58 side chain is occupied by solvent and by neighboring protein and inhibitor atoms in the mutant structure. Water molecule 220 occupies the former position of one of the Glu58 carboxyl oxygens, interacting with atom O3P of the inhibitor (Table 3). The phosphate group changes orientation in the complex of 2′-GMP with the Glu58Ala mutant (Figure 5), causing the O3P atom to overlap with the position of the Glu58 side chain in the corresponding wild-type complex. It thus appears that there is a repulsive interaction of steric or electrostatic nature between the Glu58 carboxylate and the phosphate in wild-type enzyme upon binding of 2′-GMP. A recent kinetic study also suggests that the Glu58 carboxylate disfavors binding of the dinucleoside phosphate substrate GpA (Steyaert *et al.*, 1993).

Studies of the pH dependence of the Glu58Ala RNase T1 catalyzed transesterification indicate that the reaction depends on two histidines as concerted acid/base catalysts, as is the case for RNase A (Richards & Wyckoff, 1971). His40 and His92 are located on opposite sides of the phosphate group in the present Glu58Ala RNase T1·2′-GMP structure; participation of His40 as the base catalyst along with the acid His92 is therefore compatible with the associative in-line mechanism proposed for wild-type enzyme (Eckstein *et al.*, 1972). We cannot exclude that His40 accepts the proton from 2-OH′ via the water molecule that occupies the cavity generated by the Glu58Ala substitution (see above). Crystallographic data at neutral pH may be needed to further clarify the relation between structure and mechanism for this mutant. His40 is likely to be protonated in the present structure (crystals were grown at pH 4.2, Materials and Methods), but in the catalytically active Glu58Ala enzyme species it should be deprotonated.

Glu58Ala RNase T1 crystallized in $P2_1$, and the observed protein packing differs strongly from the canonical packing of RNase T1 in $P2_12_12_1$. The effects of this change in packing on the tertiary structure of the protein are minimal: the only notable difference concerns residues Ala1 and Cys2, which are rotated over 60° around the N3–Cα3 bond, relative to the rest of the structure.

On the other hand, we observe significant changes in the solvation of the protein upon variation of its packing. Some of the water molecules associated with the protein are strictly conserved throughout the packing modes that have been investigated. A structural role can be assigned to most of these conserved water sites (see Table 4). Several water molecules stabilize the overall RNAse T1 structure by bridging different elements of the protein fold via hydrogen bonds. A striking example is the molecule in site 111 that is inaccessible to bulk solvent. Water 111 interacts with strands β1, β2, and β5 as well as with loop L4 (Figure 1). The stretch from 122 to 135 fills the space between the α-helix and a hairpin-like part of L3, while contacting only a single residue (Asp15) of the helix through hydrogen bonding. Sites 110, 124, and 133 contact single structural elements on the surface of the protein. All three water molecules provide hydrogen bonds to main-chain donor/acceptor sites that are not engaged in intramolecular contacts. It is recognized that exposure to solvent of unpaired hydrogen bond donor/acceptors stabilizes the folded state of a protein (Finney *et al.*, 1980).

However, some of the conserved sites in $P2_12_12_1$ (106, 107, 112, 113, 115, 117, 118, 119, 121, 127, 128, 129, 132; Malin *et al.*, 1991) appear to have been dictated by symmetry contacts, as these are not conserved throughout the various space groups (Table 4). All of these are situated at the surface of the protein, indicating that the primary hydration shell of a crystallized macromolecule depends strongly on packing interactions. The present study illustrates that structural data from differently packed crystals may be needed to draw meaningful conclusions on the hydration shell of a protein.

Similarly, ion binding at the surface of a protein may be space group dependent. Note that the cation binding site in the present crystal structure does not correspond to the one near Asp15, which has previously been observed in various structures in canonical space group $P2_12_12_1$ (Koepke *et al.*, 1989; Malin *et al.*, 1991). In the present structure as well as in the structures in space group $P2_12_12_1$, atoms from two neighboring protein molecules are either directly or indirectly (through the primary hydration shell) involved in ion coordination (Figure 8). A different packing may obstruct ion coordination at one site but optimize ion binding at another site. Indeed, in $P2_12_12_1$ packing, sodium binding to His92 is sterically prohibited through an intermolecular contact between the main-chain carbonyl of His92 and the amino group of Ala1 (Table 2). Inversely, Asp 15 extends into a region of bulk solvent in the present structure (see Figure 8). Hydrogen bond partners from a neighboring protein molecule that are essential to stabilize the calcium coordination shell observed in $P2_12_12_1$ (Figure 8) may be missing in space group $P2_1$.

ACKNOWLEDGMENT

We thank Dr. J. Granzin for the collection of the data and Dr. F. Körber for his excellent advice and suggestions.

REFERENCES

Altona, C., & Sundaralingam, M. (1972) *J. Am. Chem. Soc. 94*, 8205–8212.

Arni, R., Heinemann, U., Tokuoka, R., & Saenger, W. (1988) *J. Biol. Chem. 263*, 15358–15368.

Brünger, A. T., Kuriyan, J., & Karplus, M. (1987) *Science 235*, 458–460.

Crowther, R. A. (1972) in *The Molecular Replacement Method* (Rossman, M. G., Ed.) pp 173–178, Gordon & Breach, New York.

Crowther, R. A., & Blow, D. (1967) *Acta Crystallogr. 23*, 544–548.

Eckstein, F., Schultz, H., Rüterjans, H., Haar, W., & Maurer, W. (1972) *Biochemistry 11*, 3507–3512.

Finney, J. L., Gellatyl, B. J., Golton, I. C., & Goodfellow, J. (1980) *Biophys. J. 32*, 17–33.
Finzel, B. C. (1987) *J. Appl. Crystallogr. 20*, 53–55.
Fitzgerald, P. M. D. (1988) *J. Appl. Crystallogr. 21*, 273–278.
Heinemann, U., & Saenger, W. (1982) *Nature (London) 299*, 27–31.
Heinemann, U., & Polyakov, K. (1992) in *Landolt—Börnstein*, New Series (Hinz, H. J., Ed.) Springer Verlag, Berlin, Heidelberg, New York.
Hendrickson, W. A. (1985) *Methods Enzymol. 115*, 252–270.
Hendrickson, W. A., & Konnert, J. H. (1980) in *Computing in Crystallography* (Diamond, R., Ramaseshan, S., & Venkatesan, K., Eds.) pp 13.01–13.23, Indian Academy of Sciences, Bangalore.
Hill, C., Dodson, G., Heinemann, U., Saenger, W., Mitsui, Y., Nakamura, K., Borisov, S., Tischenko, G., Polyakov, K., & Pavlovsky, S. (1983) *Trends Biochem. Sci. 8*, 364–369.
Jones, T. A. (1978) *J. Appl. Crystallogr. 11*, 268–272.
Jones, T. A. (1985) *Methods Enzymol. 115*, 157–171.
Kabsch, W., & Sander, C. (1983) *Biopolymers 22*, 2577–2637.
Koellner, G., Choe, H.-W., Heinemann, U., Grunert, H.-P., Zouni, A., Hahn, U., & Saenger, W. (1992) *J. Mol. Biol. 224*, 701–713.
Koepke, J., Maslowska, M., Heinemann, U., & Saenger, W. (1989) *J. Mol. Biol. 206*, 475–488.
Kraulis, P. J. (1991) *J. Appl. Crystallogr. 24*, 946–950.
Lenz, A., Choe, H.-W., Granzin, J., Heinemann, U., & Saenger, W. (1993) *Eur. J. Biochem. 211*, 311–316.
Luzzati, V. (1952) *Acta Crystallogr. 5*, 802–810.
Malin, R., Zielenkiewicz, P., & Saenger, W. (1991) *J. Mol. Biol. 266*, 4848–4852.
Martinez-Oyanedel, J., Choe, H.-W., Heinemann, U., & Saenger, W. (1991) *J. Mol. Biol. 222*, 335–352.
Motherwell, S. (1988) PLUTO, University of Cambridge.
Nishikawa, S., Morioka, H., Kim, H., Fuchimura, K., Tanaka, T., Uesugi, S., Hakoshima, T., Tomita, K., Ohtsuka, E., & Ikehara, M. (1987) *Biochemistry 26*, 8620–8624.
Richards, F. M., & Wyckoff, H. W. (1971) in *The Enzymes*, 3rd ed. (Boyer, P., Ed.), Vol. 4, pp 647–806, Academic Press, New York.
Sato, K., & Egami, F. (1957) *J. Biochem. 44*, 753–767.
Sheriff, S. (1987) *J. Appl. Crystallogr. 20*, 55–57.
Steyaert, J., & Wyns, L. (1993) *J. Mol. Biol. 229*, 770–781.
Steyaert, J., Hallenga, K., Wyns, L., & Stanssens, P. (1990) *Biochemistry 29*, 9064–9072.
Sussman, J. L. (1985) *Methods Enzymol. 115*, 271–303.
Sussman, J. L., Holbrook, S. R., Church, G. M., & Kim, S.-H. (1977) *Acta Crystallogr. A33*, 800–804.
Zegers, I., Verhelst, P., Choe, H.-W., Steyaert, J., Heinemann, U., Saenger, W., & Wyns, L. (1992) *Biochemistry 31*, 11317–11325.